

Interplay between electronic structure and medium-range atomic order in hexagonal β -Al₉Mn₃Si and φ -Al₁₀Mn₃ crystals

Guy Trambly de Laissardière*

Laboratoire de Physique Théorique et Modélisation, CNRS / UMR 8089 – Université de Cergy-Pontoise, 95031 Cergy-Pontoise, France

(Received 24 December 2002; published 30 July 2003)

The electronic structures of the hexagonal β -Al₉Mn₃Si and φ -Al₁₀Mn₃ phases are calculated from first-principles using the TB-LMTO method. These *ab initio* results are analyzed with a simplified model for Al-based alloys containing transition metal atoms. The results show a strong effect on the atomic structure stabilization by an effective Mn-Mn interaction mediated by conduction electrons over medium-range distances (5 Å and more). The origin of large vacancies which characterize such atomic structures is explained. The position and the effect of Si atoms in stabilizing are also discussed. The atomic structures of β -Al₉Mn₃Si and φ -Al₁₀Mn₃ bear resemblance with the atomic medium-range structures of approximants of quasicrystals. Consequently, the present work gives arguments on the interplay between the medium-range atomic order and an minimization of the band energy in quasicrystals and related phases.

DOI: 10.1103/PhysRevB.68.045117

PACS number(s): 71.20.Lp, 71.23.Ft, 71.20.-b, 61.44.Br

I. INTRODUCTION

Since the 1950's, many authors¹⁻⁸ have considered Al-(rich) crystals containing transition metal (TM) atoms as Hume-Rothery alloys. In these phases, the important parameter is the average number of electrons per atom e/a . The valences of Al and Si are fixed without ambiguity (+3 and +4, respectively). Following a widely accepted model,^{5,6} a negative valence is assigned to TM atom (typically -3 for Mn, -2 for Fe, -1 for Co, and 0 for Ni). As an example, for almost isomorphic φ -Al₁₀Mn₃, β -Al₉Mn₃Si, and Al₅Co₂ phases, e/a is equal to 1.61, 1.69, and 1.86, respectively. The occurrence of different compounds with similar structures was therefore understood as Hume-Rothery phases with similar e/a ratios in spite of different atomic concentrations.⁷ In these phases, a band energy minimization occurs when the Fermi sphere touches a pseudo-Brillouin zone, spanned by Bragg vectors \mathbf{K}_p corresponding to intense peaks in the experimental diffraction pattern. The Hume-Rothery condition for alloying is then $2k_F \approx K_p$. Assuming a free electron valence band, the Fermi momentum k_F can be obtained from e/a .

The density of states (DOS) in Hume-Rothery alloys containing only *sp* valence electrons (*sp*-Hume-Rothery alloys) is correctly described by the *Jones theory* (see, for review, Refs. 9–11). The valence band (*sp* states) consists of nearly free electrons, and the scattering of electrons by the pseudo-Brillouin zone (diffraction by Bragg planes) creates a depletion in the DOS, called the “pseudogap,” near the Fermi energy E_F . The treatment of Al(rich) alloys containing TM atoms requires a different model because the *d* states of TM are not nearly free states. A model for *spd*-Hume-Rothery phases which combined the effects of the diffraction by Bragg planes with the *sp-d* hybridization has been developed.¹²⁻¹⁶ It shows that TM DOS (mainly *d* states) and the total DOS depend strongly on the positions of TM atoms.¹⁴⁻¹⁶ Indeed, some TM atoms may “fill up” the pseudogap, via the *sp-d* hybridization; whereas other TM positions enhance the pseudogap. In some particular cases, a gap is even induced by the *sp-d* hybridization.^{17,18}

The Hume-Rothery stabilization can also be viewed as a consequence of oscillating pair interactions between atoms.^{11,19-22} In this framework, Zou and Carlsson have shown^{23,24} that effective Mn-Mn interactions, mediated by *sp* states of Al, are strong enough to favor Mn-Mn distances close to 4.7 Å in Al(rich)-Mn quasicrystals and approximants. Recently,²⁵ we have shown that effective Mn-Mn interactions for distances up to 10–20 Å induce a pseudogap at E_F in cubic Al₁₂Mn, orthorhombic *o*-Al₆Mn, and cubic α -Al-Mn-Si approximant. On the other hand, this effective Mn-Mn interaction is also determinant for the existence of magnetic moments in Al-Mn quasicrystals and approximants.²⁶⁻²⁸

In this paper, an *ab initio* study of the electronic structure in β -Al₉Mn₃Si and φ -Al₁₀Mn₃ crystals is presented. Results are analyzed in the framework of Hume-Rothery mechanism for *spd* alloys. The stabilizing role of Si atoms is shown, and the effective Mn-Mn medium-range interaction allows to understand the effect of Mn positions. In particular, the origin of a large hole (vacancy Va) in both β and φ atomic structures is justified. We present the results for β , φ phases, Al₅Co₂, and μ -Al_{4,12}Mn, λ -Al₄Mn approximants. This analysis shows a strong interplay between medium-range atomic order (up to 5 Å and more) and a minimization of the band energy.

The paper is organized as follows. The structures of φ and β and their relations with medium-range atomic order of quasicrystals are discussed in Sec. II. *Ab initio* calculations, performed with the tight-binding (TB) linear muffin tin orbital (LMTO) method, are presented in Sec. III. The effect of the *sp-d* hybridization is analyzed in detail through calculations for hypothetical structures. In Sec. IV, a real space approach of the Hume-Rothery mechanism shows the strong effect of an effective medium-range Mn-Mn pair interaction (up to ~ 5 Å and more). Conclusions are given in Sec. V.

II. ATOMIC STRUCTURES

The almost isomorphic stable β -Al₉Mn₃Si (Ref. 7) and metastable φ -Al₁₀Mn₃ (Ref. 8) phases are often present in

TABLE I. Lattice parameters and atomic positions of the hexagonal β -Al₉Mn₃Si (Ref. 7), φ -Al₁₀Mn₃ (Ref. 8), and Al₅Co₂ (Ref. 29) phases from crystallographic studies. Space group is $P6_3/mmc$.

Lattice parameters		β -Al ₉ Mn ₃ Si	φ -Al ₁₀ Mn ₃	Al ₅ Co ₂
a (Å)		7.513	7.543	7.656
c (Å)		7.745	7.898	7.593
Wyckoff notation	Atomic positions	β -Al ₉ Mn ₃ Si	φ -Al ₁₀ Mn ₃	Al ₅ Co ₂
		x	z	x
			x	z
(2a)	0, 0, 0	(Al,Si)(0)	Al(0)	Al(0)
(6h)	$x, 2x, \frac{1}{4}$	(Al,Si)(1)	Al(1) 0.4579	Al(1) 0.4702
(12k)	$x, 2x, z$	(Al,Si)(2)	Al(2) 0.2006 -0.0682	Al(2) 0.1946 -0.0580
(6h)	$x, 2x, \frac{1}{4}$	Mn(1)	Mn(1) 0.1192	Co(1) 0.1268
(2d)	$\frac{2}{3}, \frac{1}{3}, \frac{1}{4}$	Va	Va	Co(0)

quenched alloys containing quasicrystals in Al(Si)-Mn systems. Their hexagonal unit cell contains 26 atoms in a complex arrangement. Unit cell dimensions of β and φ are similar (Table I), with the same space group $P6_3/mmc$. β and φ phases are almost isomorphic to Al₅Co₂,²⁹ which is an approximant of the decagonal phase.³⁰ Atomic positions and interatomic distances are given in Tables I and II.

TABLE II. Interatomic distances in β -Al₉Mn₃Si, φ -Al₁₀Mn₃, and Al₅Co₂. TM(1) is either Mn(1) or Co(1). X corresponds to the vacancy Va in β , φ phases, and to Co(0) in Al₅Co₂.

Atom	Site	Neighbors	distances (Å)		
			β -Al ₉ Mn ₃ Si	φ -Al ₁₀ Mn ₃	Al ₅ Co ₂
Al,Si(0)	(2a)	6 Al(2)	2.66	2.65	2.62
		6 TM(1)	2.48	2.53	2.53
Al(1)	(6h)	2 Al(1)	2.81	2.75	3.14
		4 Al(2)	2.77	2.84	2.74
		4 Al(2)	2.98	2.99	2.97
		2 TM(1)	2.42	2.41	2.41
		1 X	2.72	2.77	2.61
Al(2)	(12k)	1 Al,Si(0)	2.66	2.65	2.62
		2 Al(1)	2.77	2.84	2.74
		2 Al(1)	2.98	2.99	2.97
		2 Al(2)	2.81	2.79	2.73
		1 Al(2)	2.82	2.95	2.92
		2 Al(2)	2.99	3.03	3.19
		1 TM(1)	2.68	2.67	2.51
TM(1)	(6h)	2 TM(1)	2.68	2.71	2.70
		1 X	2.23	2.29	2.35
		2 Al,Si(0)	2.48	2.53	2.54
		2 Al(1)	2.42	2.41	2.41
X	(2d)	2 Al(2)	2.68	2.67	2.51
		4 Al(2)	2.68	2.71	2.70
		2 TM(1)	2.69	2.75	2.91
		3 Al(1)	2.72	2.77	2.61
		6 Al(2)	2.23	2.29	2.35
		6 TM(1) ^a	3.81	3.82	3.86

^aX and TM(1) are not first neighbors.

A. Relations with medium-range atomic order of quasicrystals

The first-neighbor atoms of Mn [Mn(1) in Table I] are 10 Al/Si + 2 Mn atoms situated at the vertices of a distorted icosahedron. Such an icosahedron is considered in the structural representation of β -Al₉Mn₃Si (Fig. 1). β -Al₉Mn₃Si and φ -Al₁₀Mn₃ structures have significant relations with the complex structures μ -Al_{4.12}Mn [hexagonal, $P6_3/mmc$, ~ 563 atoms/(unit cell)]³¹ and λ -Al₄Mn [hexagonal $P6_3/m$, ~ 568 atoms/(unit cell)]³² which are approximants with large unit cell. For instance, in Fig. 1 of Ref. 31, outlines of the repeated unit cell of φ phase on several parts of μ phase are drawn. This shows that some parts of the μ atomic structure are very similar to the atomic arrangement inside the unit cell of β , φ . Similar resemblances have been found with λ -Al₄Mn.³² Kreiner and Franzen^{32,33} have shown that the “I3 cluster,” a structure unit of three vertex connected icosahedra containing more than 30 atoms, is the basic building block of a large number of intermetallic phases related to icosahedral Al-Mn-Si such as α -Al₉Mn₂Si, μ -Al_{4.12}Mn, and λ -Al₄Mn. The I3 cluster is also found in β and φ structures.^{32,33} Therefore, although diffraction features of β and φ are different from those of quasicrystals, their atomic structure in a unit cell has important correlations with medium-range atomic order of approximants and quasicrystals.

Each Mn has two Mn first neighbors arranged in Mn triplet. Between Mn triplets, Mn-Mn distances are about 4.17 Å. Similar isolated Mn triplets exist also in μ -Al_{4.12}Mn.

B. Vacancies

The hexagonal structure of the β , φ phases is almost isomorphic to that of Al₅Co₂,²⁹ where Co replaces Mn and vacancy Va (Table I). These phases have similar atomic sites and first-neighbor distances (Table II). However, a major difference is that the site (2d) is empty (Va) in β and φ phases, whereas it is occupied by cobalt [Co(0)] in Al₅Co₂. It is thus interesting to understand why this vacancy is maintained in β and φ crystals. Because first-neighbor distances around Va in β , φ are close to those around Mn(1) in β , φ and to those around Co in Al₅Co₂, the presence of Va cannot be explained from steric encumbering.

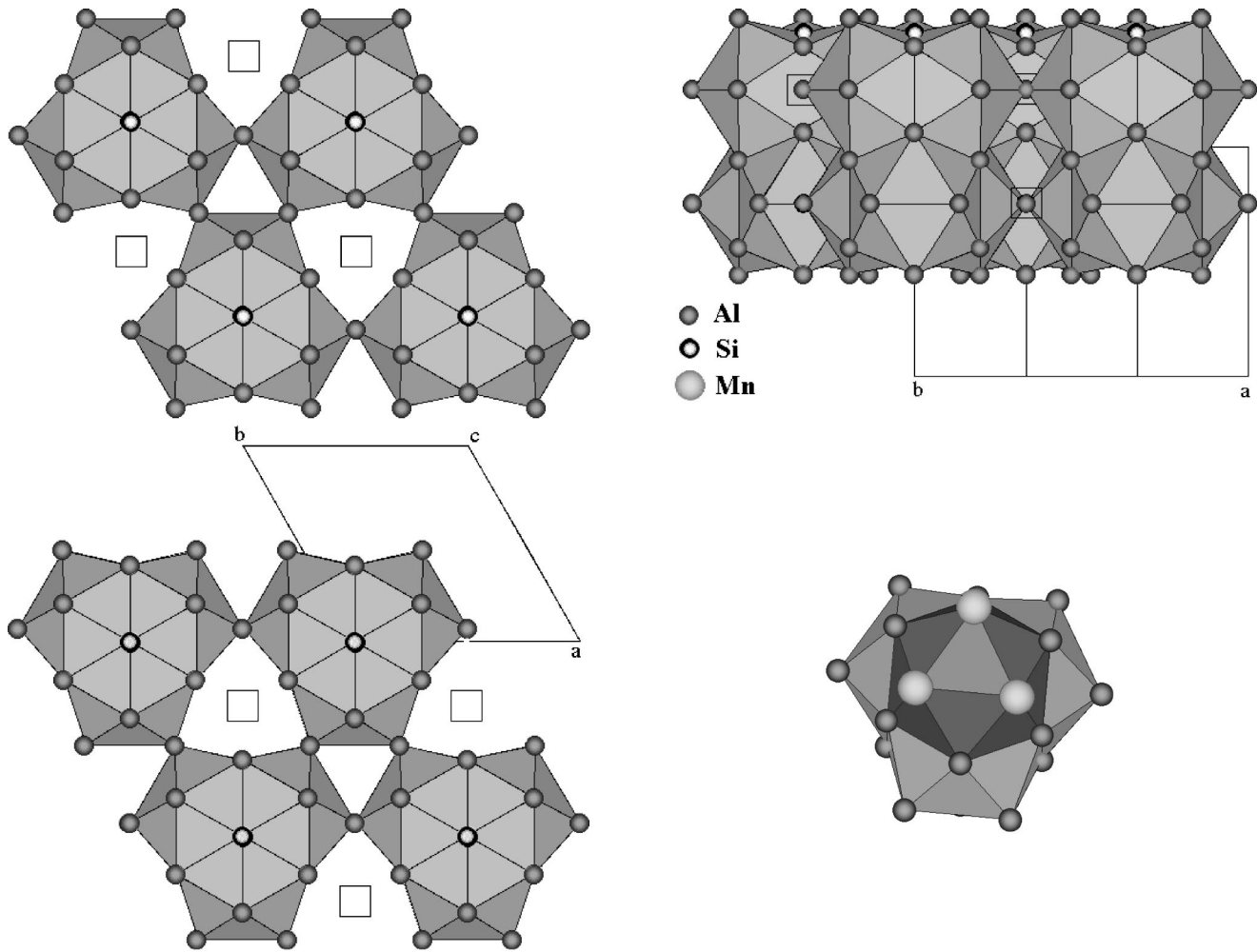


FIG. 1. Crystal structure of the β - $\text{Al}_9\text{Mn}_3\text{Si}$ phase described in terms of icosahedral clusters centered on the atoms. Si atoms are on Wyckoff site $(2a)$. Squares show the sites of the vacancy Va [site $(2d)$]. Top and side views of both layers at $z = \frac{1}{4}, \frac{3}{4}$ are shown. The icosahedral environment of each Si atom is also shown on the right low part of the figure.

Environment of Va forms a tricapped trigonal prism [3 Al(1) and 6 Al(2)]. The same environment is also found in μ - $\text{Al}_{4.12}\text{Mn}$ (Ref. 31) and λ - Al_4Mn (Ref. 32). But in μ and λ , these sites are occupied by Mn [Mn(0) site $(2b)$ in μ - $\text{Al}_{4.12}\text{Mn}$ and Mn(0) site $(2d)$ in λ - Al_4Mn]. In μ and λ , the first-neighbor distances Mn(0)-Al are 2.35–2.48 Å, which are similar to Va-Al first-neighbor distances in β and φ . In the following (Secs. III D 2 and IV C), it is shown that the presence of Va in β , φ is explained by the presence of an effective TM-TM pair interactions for distances up to medium-range distances (more than 5 Å).

C. Role and positions of Si atoms

A small proportion of Si atoms is known to have strong effect in stabilizing Al-based phases. Unstable quasicrystals are obtained in Al-Mn system, whereas stable quasicrystals are formed when a small proportion of Si atoms is added.^{34,35} Similar stabilizing effects occur for icosahedral Al-Cu-Cr-Si,³⁶ and for the approximants α -Al-Mn-Si,³⁴

$1/1$ Al-Cu-Fe-Si,^{37,38} and α -Al-Re-Si.³⁹ Investigations on the relations between isomorphous stable β - $\text{Al}_9\text{Mn}_3\text{Si}$ and metastable φ - $\text{Al}_{10}\text{Mn}_3$ phases represent thus a great interest in order to analyze Si effect. The number of valence electrons are 3 (4) per Al (Si) atom. With respect to the Hume-Rothery condition for alloying ($2k_F \approx K_p$), it may be possible that the substitution of a small quantity of Si increases the e/a ratio, which is in better agreement with $2k_F \approx K_p$.

Experimentally, Al and Si atoms have not been distinguished in β - $\text{Al}_9\text{Mn}_3\text{Si}$. However, Robinson⁷ has proposed that Si atoms are on site $(2a)$ because the interatomic distances between an atom in $(2a)$ and its six neighboring Al atoms are less than the distances between any other pairs of Al atoms in β structure (Table II). But, from a comparison of β and φ , Taylor⁸ has suggested that Si atoms should be preferentially in $(12k)$ instead of in $(2a)$. In this case, Si site has mixed occupancy with some Al. In Sec. III, an analysis of *ab initio* calculations suggests that Si atoms are likely to be in $(2a)$.

III. AB INITIO CALCULATIONS OF THE ELECTRONIC STRUCTURE

A. LMTO procedure, treatment of Si

Electronic structure determinations are performed in the framework of the local spin-density approximation (LSDA)⁴⁰ by using the self-consistent tight-binding (TB) linear muffin tin orbital (LMTO) method [TB-LMTO Version 4.6 (1994), O. K. Andersen, Stuttgart, Germany].^{41,42} In the atomic sphere approximation (ASA),^{41,42} space is divided into atomic spheres and interstitial regions where the potential is respectively spherically symmetric and flat. Following the standard procedure, sphere radii are chosen so that the total volume of atomic (Wigner-Seitz) spheres is equal to that of the solid. This code includes combined corrections that correct errors from the partial overlap of the spheres and interstitial regions in ASA. For vacancies (Va) empty spheres are introduced on site (2d). The sphere radii (R) are determined so as to minimize the overlap between spheres: $R_{\text{Si/Al}(0)} = 1.37 \text{ \AA}$, $R_{\text{Al}(1)} = R_{\text{Al}(2)} = 1.53 \text{ \AA}$, $R_{\text{Mn}} = 1.34 \text{ \AA}$, $R_{\text{Va}} = 1.04 \text{ \AA}$ for β phase, and $R_{\text{Al}(0)} = 1.38 \text{ \AA}$, $R_{\text{Al}(1)} = R_{\text{Al}(2)} = 1.55 \text{ \AA}$, $R_{\text{Mn}} = 1.35 \text{ \AA}$, $R_{\text{Va}} = 1.05 \text{ \AA}$ for φ phase. As these structures are metallic and rather compact, it is found that a small change of sphere radii (less than 10%) does not modify significantly the results. Neglecting the spin-orbit coupling, a scalar relativistic LMTO-ASA code is used. Electronic densities of states (DOS's) are calculated by integration on a reduced Brillouin zone.⁴³ The final step of the self-consistent procedure and the DOS calculation are performed with 4416 \mathbf{k} points in the reduced Brillouin zone. With an energy mesh equal to $\Delta E = 0.09 \text{ eV}$, the calculated DOS's do not exhibit significant differences when the number of \mathbf{k} points increases from 2160 to 4416. The energy accuracy is thus less than 0.09 eV and details in DOSs larger than 0.09 eV are not artifacts in calculations. In LMTO DOS figures the energy resolution is equal to 0.09 eV.

The LMTO basis includes all angular momenta up to $l = 2$ and the valence states are Al ($3s, 3p, 3d$), Mn ($4s, 4p, 3d$), Co ($4s, 4p, 3d$), Si ($3s, 3p, 3d$) and Va ($1s, 2p, 3d$).⁴⁴ In order to analyze the position of Si atoms in the β phase, we perform calculations for $\beta\text{-}(\text{Al}, \text{Si})_{10}\text{Mn}_3$ where the Si atoms occupied randomly the Al sites. In this case an average atom, named (Al,Si), is considered (virtual crystal approximation). In the LMTO-ASA procedure this atom is simulated by an atom with nuclear charge $Z = (1 - c)Z_{\text{Al}} + cZ_{\text{Si}}$, where c is the proportion of Si atoms, and $Z_{\text{Al}} = 13$, $Z_{\text{Si}} = 14$ are the nuclear charge of Al, Si, respectively. Such a calculation is justified because the main difference between Al and Si is the number of valence electrons. Three possibilities are considered for the β phase.

The phase called $\beta\text{-Al}_9\text{Mn}_3\text{Si}$ where Si are on site (2a) and Al, on site (6h) and site (12k) as proposed by Robinson.⁷

The phase $\beta\text{-I}(\text{Al}, \text{Si})_{10}\text{Mn}_3$ where Si atoms substitute for some Al on sites (2a), (6h), and (12k).

The phase $\beta\text{-II}(\text{Al}, \text{Si})_{10}\text{Mn}_3$ where Si atoms substitute for some Al(2) [site (12k)] as proposed by Taylor.⁸

For these three cases, the same atomic positions and sphere radii are assumed.

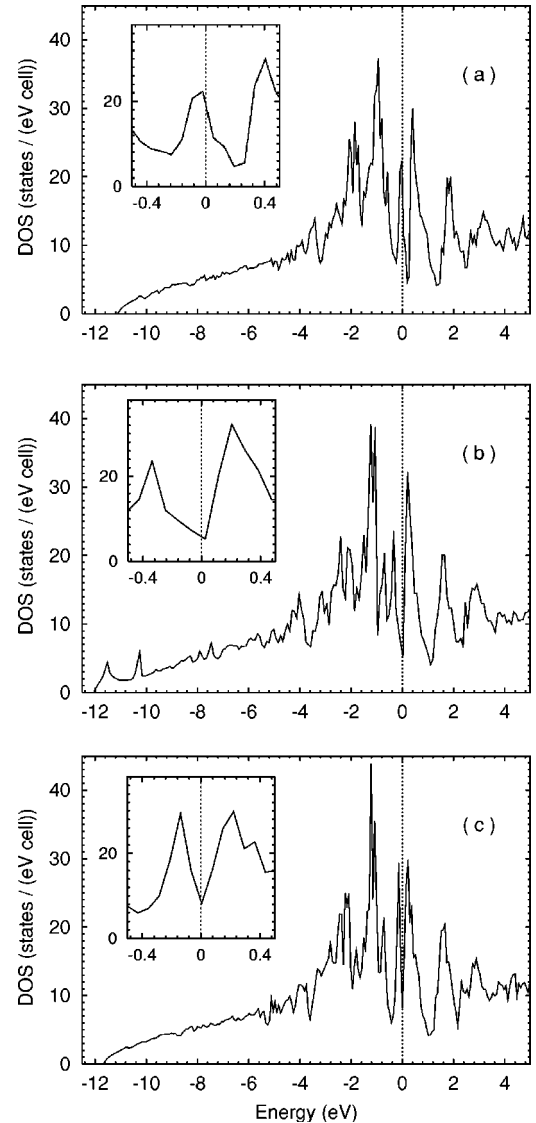


FIG. 2. Total density of states (DOS) calculated by LMTO-ASA method of (a) $\varphi\text{-Al}_{10}\text{Mn}_3$, (b) $\beta\text{-Al}_9\text{Mn}_3\text{Si}$, and (c) $\beta\text{-I}(\text{Al}, \text{Si})_{10}\text{Mn}_3$. Details of the total DOS's around E_F are given in the insets. $E_F = 0$. The DOS of $\beta\text{-II}(\text{Al}, \text{Si})_{10}\text{Mn}_3$ is almost the same than that of $\beta\text{-I}(\text{Al}, \text{Si})_{10}\text{Mn}_3$.

B. General aspects of the density of states (DOS)

Self-consistent total energies are calculated for different volumes, with isotropic volume changes, i.e., the ratio c/a is constant and equal to the experimental value (Table I). The atomic positions are not relaxed. Minima of energies are obtained for nonmagnetic Mn (paramagnetic states). Calculated lattice parameters a are equal to 7.41 \AA for $\beta\text{-Al}_9\text{Mn}_3\text{Si}$, 7.41 \AA for $\beta\text{-I}(\text{Al}, \text{Si})_{10}\text{Mn}_3$, 7.42 \AA for $\beta\text{-II}(\text{Al}, \text{Si})_{10}\text{Mn}_3$, and 7.43 \AA for $\varphi\text{-Al}_{10}\text{Mn}_3$. These values are, within 1.5%, close to experimental values (Table I). Similar results have also been found in LMTO-ASA calculations for Al-TM crystals with a small concentration of TM elements.¹⁵

The total DOSs of β and φ phases (Fig. 2), are very similar. Local DOS's of β are also shown Fig. 3. Except for low energies (less than -10 eV), the total DOS of β does not depend on Si positions. The parabola due to the Al nearly

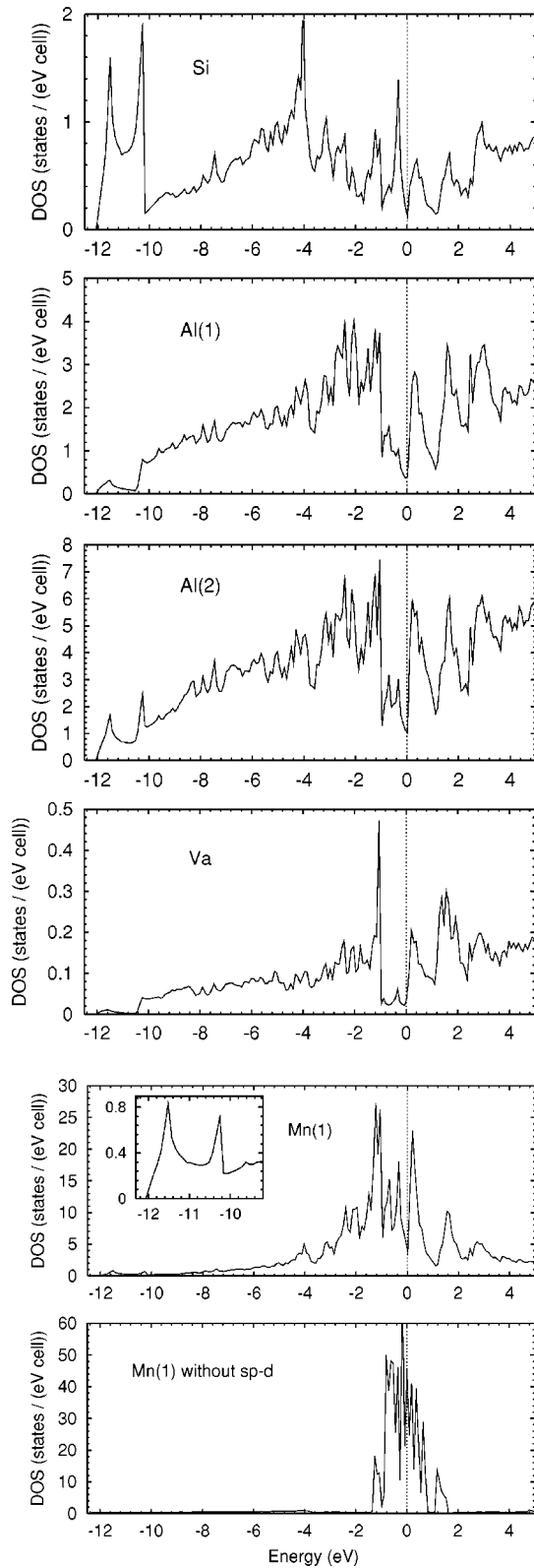


FIG. 3. LMTD local DOSs of $\beta\text{-Al}_9\text{Mn}_3\text{Si}$ phase. Si atoms are on Wyckoff sites (2a). The local Mn(1) DOS calculated without sp - d hybridization is also shown (see text). $E_F=0$.

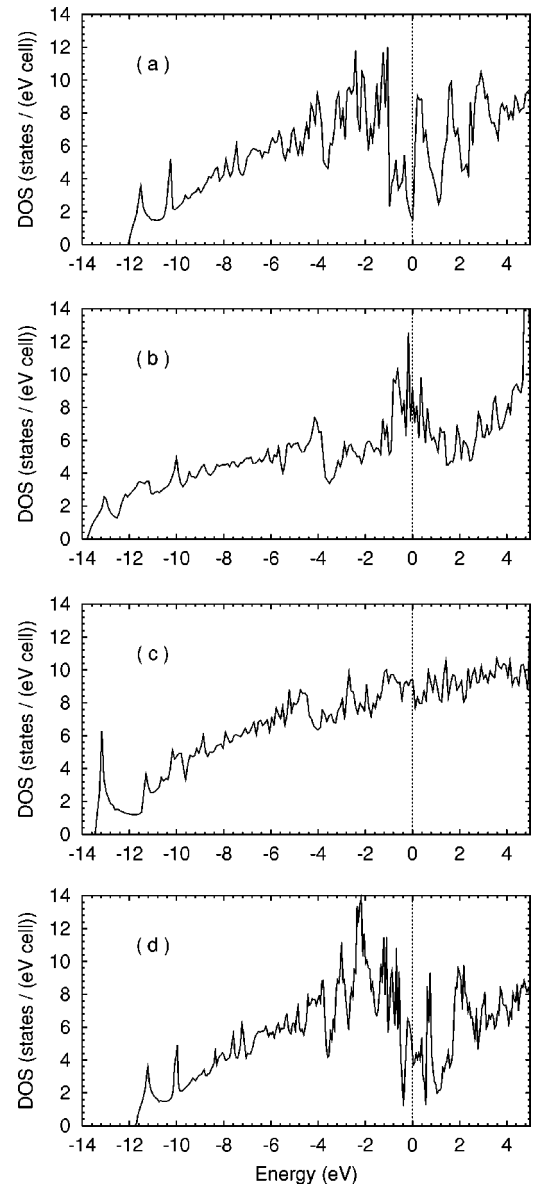


FIG. 4. LMTD local {Al + Si} DOS of $\beta\text{-Al}_9\text{Mn}_3\text{Si}$: (a) calculated including sp - d hybridization, (b) calculated without sp - d hybridization. (c) Local {Al + Si} DOS of hypothetical $\beta\text{-Al}_9\text{Al}_3\text{Si}$ and (d) of hypothetical $\beta\text{-Al}_9\text{Mn}_4\text{Si}$. $E_F=0$.

free states is clearly seen. A large d band, from -2 to 2 eV, is due to a strong sp - d hybridization in agreement with experimental results^{45–49} and with *ab initio* calculations^{15,50–52} for Al-TM crystals and quasicrystals.

The sum of local DOS's on Al and Si atoms, shown Fig. 4(a), is mainly a sp DOS. As expected for a Hume-Rothery stabilization, it exhibits a wide pseudogap near E_F due to electron scattering by Bragg planes of a pseudo-Brillouin zone. The width of the pseudogap in {Al + Si} DOS is about 1 eV. This is the same order of magnitude as the one found in Al-Mn icosahedral approximants.^{15,50–52} This large pseudogap is mainly characteristic of a p band at this energy, but the pseudogap in the total DOS is narrower. Indeed d states of Mn atoms fill up partially the pseudogap in the total DOS [Fig. 2(b)] with respect to the pseudogap in {Al + Si}

DOS [Fig. 4(a)]. Nevertheless, it is shown in the following that the presence of a pseudogap in $\{\text{Al} + \text{Si}\}$ DOS is related to the scattering of sp states by the Mn sublattice via the $sp-d$ hybridization.

Spiky DOS's were obtained for the studied phases as it has been found in LMTO DOS of icosahedral small approximants [α -Al-Mn-Si,⁵⁰ 1/1 Al-Cu-Fe,⁵¹ 1/1 Al-Pd-Mn (Ref. 53)]. It is the small electron velocity (flat dispersion relations) which contributes to anomalous electronic transport properties.^{50,51,54} It may come from long-range atomic order and/or medium-range atomic order. Fine peaks in the DOS may be the signature of electron confinements⁵⁵ in atomic clusters characteristic⁵⁶ of the quasiperiodicity. This is not in contradiction to a Hume-Rothery mechanism because this tendency to localization has a small effect on the band energy.⁵⁵ The existence of spiky DOSs in quasicrystals is much debated experimentally^{57,59,60} and theoretically (Ref. 58, and references therein). Our calculations do not give an answer to this question in the case of quasicrystals. But for β and φ crystals, we have checked that features in DOS with an energy resolution equal to 0.09 eV are not artifacts in calculations (Sec. III A).

C. Analysis of Si effect

The total DOS's of β -I-(Al,Si)₁₀Mn₃ [Si mixed with Al on sites (2a), (6h), and (12k)] and β -II-(Al,Si)₁₀Mn₃ [Si mixed with Al on site (12k)] are very similar, thus we present only those of β -I-(Al,Si)₁₀Mn₃ [Fig. 2(c)]. In the vicinity of E_F , this DOS is rather similar to the DOS of β -Al₉Mn₃Si [Si are in (2a)]. In particular, E_F is always located at the minimum of the pseudogap as expected in a Hume-Rothery stabilization.

Nevertheless, a difference between the band energy of β -(Al,Si)₁₀Mn₃ and that of β Al₉Mn₃Si is shown from LMTO DOS's. Two bonding peaks are present at low energies (-11.5 and -10.3 eV, Fig. 3) in the local Si DOS of β -Al₉Mn₃Si. Each Si atom has 6 Al(2) and 6 Mn first neighbors (Table II). The close proximity between Si and Mn(1) and the presence of the two peaks in Mn(1) DOS at the same energies show that the Si-Mn(1) bond is rather strong. This suggests a covalent character of the Si-Mn(1) bond which increases the stability of β phase when Si are in (2a).

In the vicinity of E_F , the total DOSs of β -Al₉Mn₃Si and φ -Al₁₀Mn₃ are similar except the position of E_F [Figs. 2(a) and 2(b)]. At E_F , the DOS of β is 5.6 states/(eV unit cell), and the DOS of φ , 16.0 states/(eV unit cell). The small amount of Si increases the average valence e/a in β . As in a rigid band model, E_F is moved to the minimum of the pseudogap, and the band energy is thus minimized. This allows us to understand why the β -Al₉Mn₃Si phase is stable whereas the φ -Al₁₀Mn₃ phase is metastable.

D. Effects of the d states of the transition-metal atoms

In this part the origin of the pseudogap is analyzed from LMTO calculations for hypothetical phases derived from β -Al₉Mn₃Si. Three points are successively considered: (1) the effect on the pseudogap of the $sp-d$ hybridization, (2) the

role of Mn positions which explains the origin of the vacancy (Va) in β and φ phases, and (3) the effect on the pseudogap of Mn-Mn pair distances up to 5 Å and more.

1. Role of the $sp-d$ hybridization on the pseudogap

Self-consistent LMTO calculations are performed without $sp-d$ hybridization by setting to zero the corresponding terms of the hamiltonian matrix.¹⁷ Such a calculation is physically meaningful because the Mn d states are mainly localized in the Mn sphere and the Al sp states are delocalized. In Fig. 3, the local Mn DOS (mainly d states) is shown in two cases: with $sp-d$ hybridization and without $sp-d$ hybridization. The comparison between these local DOSs shows that the $sp-d$ hybridization increases the width of the d band. This confirms a strong $sp-d$ hybridization. The local $\{\text{Al} + \text{Si}\}$ DOS [mainly sp DOS, Fig. 4(a)] is also affected by the $sp-d$ hybridization since the pseudogap disappears completely in the calculation without $sp-d$ hybridization [Fig. 4(b)].

For Hume-Rothery alloys containing TM elements, a stabilization mechanism is more complex than for sp alloys because of the important $sp-d$ hybridization in the vicinity of E_F .^{14,15} Al and Si atoms, which have a weak potential V_B , scatter sp electrons by a potential almost energy independent. This leads to the so-called diffraction of electrons by Bragg planes in sp alloys (Jones theory).^{9-11,22} But, the potential of Mn atoms depends on the energy. It is strong for energies around E_d , and thus creates a d resonance of the wave function which scatters sp states via the $sp-d$ hybridization. Therefore in β , φ phases, the scattering by the Mn(1) sublattice creates a Hume-Rothery pseudogap.

LMTO calculations performed for hypothetical β -Al₉Al₃Si, constructed by putting Al in place of Mn(1) in β -Al₉Mn₃Si, confirm the previous analysis. There are many small depletions in the DOS of hypothetical β -Al₉Al₃Si [Fig. 4(c)] that may come from diffraction by Bragg planes. But there is no longer a pronounced pseudogap near E_F . This shows that electron diffraction by Bragg planes by a weak potential V_B is not enough to explain the pseudogap in DOSs of β -Al₉Mn₃Si and φ -Al₁₀Mn₃.

2. Effect of Mn positions, origin of the vacancy

As explained in Sec. II, a particularity of β and φ structures is a vacancy Va on site (2d). This is the main difference with the Al₅Co₂ structure (Table I). The origin of this vacancy cannot be explained from small near-neighbor distances (Sec. II B). LMTO calculations are performed including a new Mn atom, called Mn(0), on site (2d) in β -Al₉Mn₃Si phase. Atomic positions and lattice parameters are those of β -Al₉Mn₃Si (Table I). This hypothetical phase is named β -Al₉Mn₄Si. Its total DOS and $\{\text{Al} + \text{Si}\}$ DOS are shown Figs. 5 and 4(d), respectively.

The absence of pseudogap in the total DOS shows a great effect Mn(0) which is very different from the one of Mn(1) analyzed previously. Indeed Mn(1) [on site (6h)] creates the pseudogap in β -Al₉Mn₃Si DOS, whereas Mn(0) destroys it in hypothetical β -Al₉Mn₄Si total DOS. In local $\{\text{Al} + \text{Si}\}$ DOS [Fig. 4(d)] a pseudogap is still present. It comes from the scattering by Mn(1) atoms. But a large peak fills up

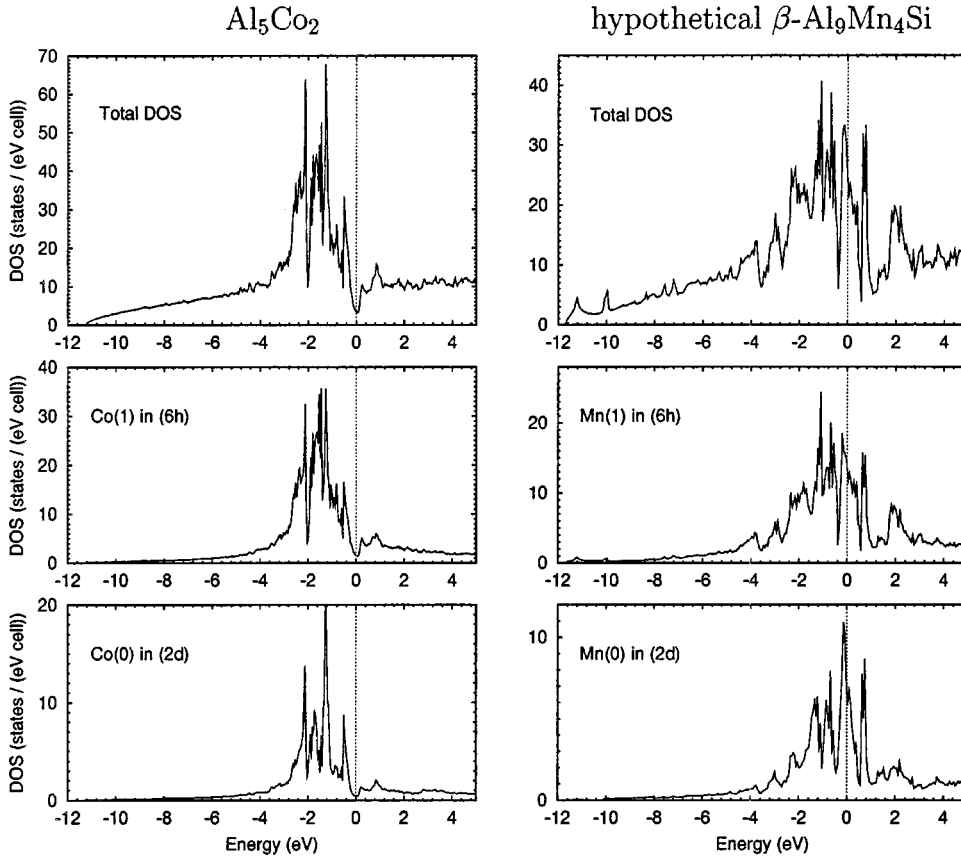


FIG. 5. LMTO total DOS's and local TM DOS's of Al_5Co_2 and hypothetical $\beta\text{-Al}_9\text{Mn}_4\text{Si}$. The $\beta\text{-Al}_9\text{Mn}_4\text{Si}$ phase is built from $\beta\text{-Al}_9\text{Mn}_3\text{Si}$ (Table I) by replacing the vacancy in (2d) by Mn atom [Mn(0)]. $E_F=0$.

partially this pseudogap in hypothetical $\beta\text{-Al}_9\text{Mn}_4\text{Si}$ DOS. Consequently, E_F is located in an antibonding peak due to $sp[\text{Al}]-d[\text{Mn}(0)]$ hybridization. Thus Mn(0) on site (2d) “fills up” the pseudogap via the $sp-d$ hybridization; whereas Mn(1) on site (6h) enhances the pseudogap. A similar result is obtained for hypothetical $\varphi\text{-Al}_{10}\text{Mn}_4$, by putting Mn(0) in place of the vacancy in (2d). This illustrates clearly the non-trivial effect of the Mn positions on the electronic structure of spd -Hume-Rothery alloys.^{14,15}

Total and local DOS's of hypothetical $\beta\text{-Al}_9\text{Mn}_4\text{Si}$ and Al_5Co_2 (Refs. 15,46) are compared in Fig. 5. In spite of the same proportion of TM atoms and the near isomorphism between these structures, their DOS's are very different. There is pseudogap in Al_5Co_2 DOS and not in $\beta\text{-Al}_9\text{Mn}_4\text{Si}$ DOS. This indicates that Co(0) and Mn(0) act differently, thus justify the existence of a vacancy in both $\beta\text{-Al}_9\text{Mn}_3\text{Si}$ and $\varphi\text{-Al}_{10}\text{Mn}_3$ phases but not in Al_5Co_2 . Similar Wyckoff sites (2d) lead to both antibonding or bonding peaks depending on the nature of the atom on this site [either Mn(0) or Co(0), respectively]. A further analysis is proposed in Sec. IV, where cohesive energies are compared using realistic TM-TM pair interactions.

3. Effect of Mn-Mn distances close to 5 Å

Mn-Mn distances in $\beta\text{-Al}_9\text{Mn}_3\text{Si}$ are reported in Table III. Mn are grouped together to form Mn triplets (Sec. II A). In order to determine the effect of an effective Mn-Mn interaction on the pseudogap, LMTO calculations are performed for a modified β phase containing only one Mn-triplet per unit

cell instead of two. $\beta\text{-Al}_9\text{Mn}_3\text{Si}$ was thus transformed into $\beta\text{-Al}_9\text{Mn}_{1.5}\text{Cu}_{1.5}\text{Si}$ by replacing one Mn triplet by one Cu triplet. Mn environments remain identical up to 4.17 Å (Table III).

The local Cu DOS at E_F is very small [Fig. 6(d)]. Cu having almost the same number of sp electrons as Mn, it has then a minor effect near E_F . The pseudogap disappears completely in local Mn DOS [Fig. 6(c)]. A small depletion below E_F is still remaining in total DOS [Fig. 6(a)]. There is a pseudogap below E_F in local $\{\text{Al} + \text{Si}\}$ DOS [Fig. 6(b)], but it is less pronounced than for $\beta\text{-Al}_9\text{Mn}_3\text{Si}$ [Fig. 4(a)]. Such a disappearance of the pseudogap is due to the effect of an effective Mn-Mn interaction for distances equal to 4.17, 4.96, and 6.38 Å (. . .) (Table III).

TABLE III. Mn-Mn distances in $\beta\text{-Al}_9\text{Mn}_3\text{Si}$ and hypothetical $\beta\text{-Al}_9\text{Mn}_{1.5}\text{Cu}_{1.5}\text{Si}$ (see text).

Mn-Mn distance (Å)	Number of Mn-Mn pairs	
	$\beta\text{-Al}_9\text{Mn}_3\text{Si}$	$\beta\text{-Al}_9\text{Mn}_{1.5}\text{Cu}_{1.5}\text{Si}$
2.69	2	2
4.17	4	
4.83	2	2
4.96	2	
6.38	4	
6.59	4	4
7.33	8	
7.51	6	6

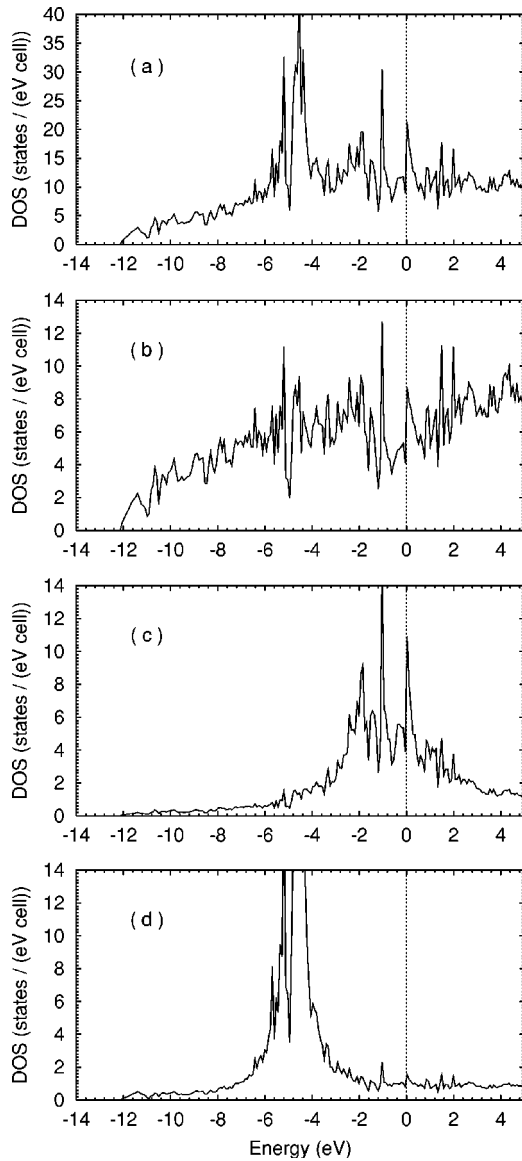


FIG. 6. LMTO DOS's of hypothetical β -Al₉Mn_{1.5}Cu_{1.5}Si: (a) total DOS, (b) {Al + Si} local DOS, (c) Mn local DOS, (d) Cu local DOS. The hypothetical β -Al₉Mn_{1.5}Cu_{1.5}Si is built by replacing one Mn triplet by one Cu triplet in each unit cell of β -Al₉Mn₃Si. $E_F = 0$.

IV. ROLE OF EFFECTIVE MN-MN INTERACTION ON THE ATOMIC STRUCTURE

A. Medium-range TM-TM interaction in Al based alloys

Since Blandin¹⁹ the Hume-Rothery stabilization can be explained in the framework of the pseudopotential theory.^{9,11,20–22} In this method, the energy is the sum of a term E_0 (which depends on the electronic density alone) and of a term E_{BS} (which depends on positions of the atoms). E_0 represents about 80 to 90 % of the total energy, and it is essential in fixing the average atomic density. E_{BS} can be written as a sum of atomic pair interactions Φ_{A-B} which present medium-range Friedel oscillations. A Hume-Rothery stabilization is thus a consequence of the oscillations of Φ . Realistic pair interactions^{23,24,61,62} have been used success-

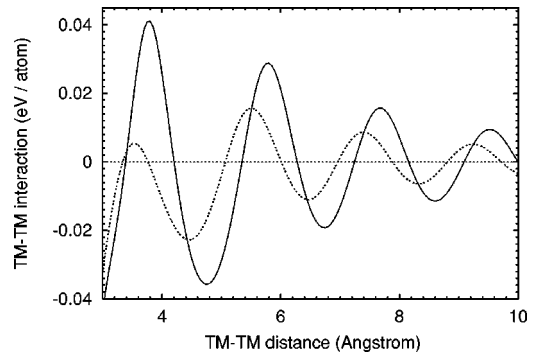


FIG. 7. Effective medium-range TM-TM pair interactions: (solid lines) Mn-Mn interaction $\Phi_{\text{Mn-Mn}}$ and (dashed line) Co-Co interaction $\Phi_{\text{Co-Co}}$. These interactions do not include short range repulsive terms between two TM atoms. TM atoms are nonmagnetic.

fully for molecular-dynamics studies^{63,64} of Al-Mn and Al-Co phases with composition close to those of quasicrystals. Because the magnitude of the pseudopotential of TM atoms is stronger than those of Al and Si, it follows that the magnitude of $\Phi_{\text{TM-TM}}$ is larger than those of $\Phi_{\text{Al-TM}}$ and $\Phi_{\text{Al-Al}}$. Zou and Carlsson^{23,24} have shown the existence of a specific Mn-Mn distance equals to 4.7 Å in Al(rich)-Mn phases. A TM-TM interaction may thus play a significant role in the stabilization. This interaction is mediated by the sp states of Al, via the strong $sp(\text{Al})-d(\text{TM})$ hybridization. Consequently, this is a medium-range interaction (Fig. 7). Let us remark that the role of Al atoms is essential; indeed, without $sp(\text{Al})-d(\text{TM})$ hybridization the TM-TM interaction should be only a short-range interaction (\sim first-neighbor interaction). This is the reason why we named this TM-TM interaction an “effective” interaction. Our calculations⁵⁵ of $\Phi_{\text{Mn-Mn}}$ and $\Phi_{\text{Co-Co}}$ (Fig. 7), performed within a multiple scattering approach, yield results which are in good agreement with those given in Ref. 23. Parameters in these calculations are the Fermi level E_F fixed by the Al matrix ($E_F = 11.7$ eV), the width 2Γ of the d resonance which increases as the $sp-d$ hybridization increases, and the energy E_d of the d resonance. For Mn, realistic values are $2\Gamma = 2.7$ eV, $E_d = 11.37$ eV; and for Co, $2\Gamma = 2$ eV, $E_d = 10.6$ eV. We have checked that a small variation of these parameters does not modify qualitatively the results presented in the following.

The magnitude of the effective interaction is larger for Mn pair than for other TM pairs (TM=Cr, Fe, Co, Ni), because the number of d electrons with energy close to E_F is the largest for Mn. Indeed, electrons at Fermi energy are the most delocalized electrons and thus they contribute more to the medium-range interaction. From Fig. 7, it is clear that distances corresponding to minima of $\Phi_{\text{TM-TM}}$ depend also on the nature of TM atom.

B. Contribution to the total energy of the effective Mn-Mn interaction

The “structural energy” \mathcal{E} of TM sublattice in Al(Si) host is defined as the energy needed to build the TM sub-lattice in the metallic host from isolated TM atoms in the same metal-

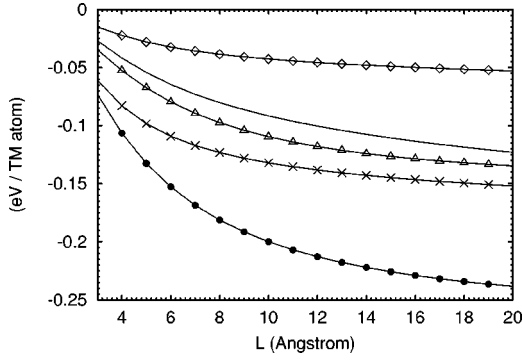


FIG. 8. Structural energy \mathcal{E}' of the Mn sublattice in (line) β - $\text{Al}_9\text{Mn}_3\text{Si}$, (Δ) φ - $\text{Al}_{10}\text{Mn}_3$, (\bullet) o - Al_6Mn , (\times) α - Al-Mn-Si , and (\diamond) hypothetical β - $\text{Al}_9\text{Mn}_{1.5}\text{Cu}_{1.5}\text{Si}$.

lic host. The metallic host is a jellium which models Al and Si atoms. The \mathcal{E} per unit cell is

$$\mathcal{E} = \sum_{i,j(j \neq i)} \frac{1}{2} \Phi_{\text{TM-TM}}(r_{ij}) e^{-r_{ij}/L}, \quad (1)$$

where i and j are the indices of TM atoms and r_{ij} , the TM(i)-TM(j) distances. L is the mean-free path of electrons due to scattering by static disorder or phonons.⁶⁵ L depends on structural quality and temperature, and it is estimated to be larger than 10 Å. Note that a similar exponential damping factor was introduced originally in the treatment of RKKY interaction.^{19,66} In the following, the effects of TM-TM pairs for distances larger than first-neighbor distances are analyzed. Therefore, an energy \mathcal{E}' is calculated from Eq. (1) without including the first-neighbor TM-TM terms in the sum. \mathcal{E}' is the part of the structural energy of TM sublattice that comes only from indirect TM-TM interactions.

Structural energies \mathcal{E}' of the Mn sublattice are shown for β - $\text{Al}_9\text{Mn}_3\text{Si}$ and φ - $\text{Al}_{10}\text{Mn}_3$ structures in Fig. 8. They are compared to those of o - Al_6Mn ,⁶⁷ and α - Al-Mn-Si approximants.^{68,69} \mathcal{E}' is always negative with magnitudes less than -0.1 eV/Mn atom. This is strong enough to give a significant contribution to the minimization of the band energy.

This result is in good agreement with the effect of Mn sublattice on the pseudogap shown previously (Sec. III D). According to a Hume-Rothery mechanism, one expects the pseudogap to be well pronounced for a large value of $-\mathcal{E}'$. Such a correlation is verified for the hypothetical β - $\text{Al}_9\text{Mn}_{1.5}\text{Cu}_{1.5}\text{Si}$ (Sec. III D 3). Indeed the decrease of the pseudogap in β - $\text{Al}_9\text{Mn}_{1.5}\text{Cu}_{1.5}\text{Si}$ sp DOS [Fig. 6(b)] as compared to the pseudogap in β - $\text{Al}_9\text{Mn}_3\text{Si}$ sp DOS [Fig. 4(a)] corresponds to a reduction of $-\mathcal{E}'$ (Fig. 8).

C. Origin of the vacancy

For phases containing several TM Wyckoff sites, the effective TM-TM interactions allow us to compare the relative stability of TM atoms on different Wyckoff sites. Considering a phase with a structural energy of the TM sublattice equal to \mathcal{E} , the variation $\Delta\mathcal{E}'_i$ of \mathcal{E} is determined when one TM(i) atom is removed from the structure

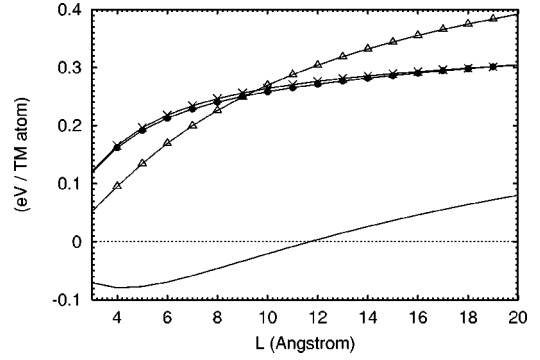


FIG. 9. Variation of the structural energy $\Delta\mathcal{E}'_i$ due to Mn-Mn interactions for (simple line) Mn(0) in (2d) in the hypothetical β - $\text{Al}_9\text{Mn}_4\text{Si}$; for (Δ) Mn(1) in (6h) in the hypothetical β - $\text{Al}_9\text{Mn}_4\text{Si}$; for (\bullet) Mn(0) in (2b) in μ - $\text{Al}_{4.12}\text{Mn}$; and for (\times) Mn(0) in (2d) in λ - Al_4Mn . Mn(0) in hypothetical β - $\text{Al}_9\text{Mn}_4\text{Si}$, μ - $\text{Al}_{4.12}\text{Mn}$, and λ - Al_4Mn have similar local environments.

$$\Delta\mathcal{E}'_i = - \sum_{j(j \neq i)} \Phi_{\text{TM-TM}}(r_{ij}) e^{-r_{ij}/L}. \quad (2)$$

The TM atoms on different Wyckoff sites have different $\Delta\mathcal{E}'_i$ values. The most stable TM sites correspond to the highest $\Delta\mathcal{E}'_i$ values. The energy reference is one TM impurity in the Al(Si) matrix which does not depend on the structure. Therefore, it is possible to compare the $\Delta\mathcal{E}'_i$ calculated for TM atoms of different phases. As previously, the energy $\Delta\mathcal{E}'_i$ is calculated from Eq. (2) without the first-neighbor TM-TM contributions in order to analyze effects at medium-range order.

For the hypothetical β - $\text{Al}_9\text{Mn}_4\text{Si}$, built from β - $\text{Al}_9\text{Mn}_3\text{Si}$ where Mn(0) replaces the vacancy on site (2d) [Sec. III D 2], it appears that $\Delta\mathcal{E}'_{\text{Mn}(1)} > \Delta\mathcal{E}'_{\text{Mn}(0)}$ (Fig. 9). Mn(0) in (2d) is therefore less stable than Mn(1) in (6h) in the hypothetical β - $\text{Al}_9\text{Mn}_4\text{Si}$, thus this justifies that a vacancy exists in the actual β phase. A similar result is obtained for an hypothetical φ - $\text{Al}_{10}\text{Mn}_4$, by putting Mn(0) in place of the vacancy in (2d).

On the contrary, the complex μ - $\text{Al}_{4.12}\text{Mn}$ and λ - Al_4Mn crystals contain a Mn site [site (2b) in μ - $\text{Al}_{4.12}\text{Mn}$ (Ref. 31) and site (2d) λ - Al_4Mn (Ref. 32)] with a local environment similar to Va [or Mn(0)] environment in β structure (Sec. II B). We name Mn(0) the Mn atoms on these sites in μ and λ phases. As shown Fig. 9, the corresponding $\Delta\mathcal{E}'_{\text{Mn}(0)}$ values differ strongly from those of Mn(0) in hypothetical β - $\text{Al}_9\text{Mn}_4\text{Si}$:

$$\Delta\mathcal{E}'_{\text{Mn}(0)}(\mu) \approx \Delta\mathcal{E}'_{\text{Mn}(0)}(\lambda) > \Delta\mathcal{E}'_{\text{Mn}(0)}(\beta) \approx \Delta\mathcal{E}'_{\text{Mn}(0)}(\varphi). \quad (3)$$

Thus, Mn(0) atom is more stable in μ - $\text{Al}_{4.12}\text{Mn}$ and λ - Al_4Mn than Mn(0) in hypothetical β - $\text{Al}_9\text{Mn}_4\text{Si}$ and hypothetical φ - $\text{Al}_{10}\text{Mn}_4$. Moreover, $\Delta\mathcal{E}'_{\text{Mn}(0)}$ in μ (λ) have the same order of magnitude as the energy $\Delta\mathcal{E}'_i$ calculated for other Mn(i) atoms in μ (λ) (μ and λ phases contain 10 and 15 Mn Wyckoff sites, respectively). Therefore as far as the effective Mn-Mn interaction is concerned, Mn(0) in μ and λ are as stable as other Mn in these phases. Such a difference

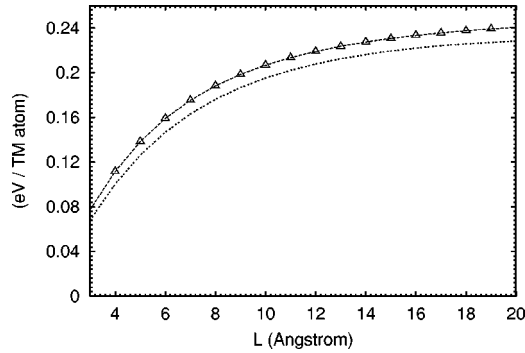


FIG. 10. Variation of the structural energy $\Delta\mathcal{E}'_i$ due to Co-Co interactions in Al_5Co_2 . $\Delta\mathcal{E}'_i$ is calculated for the two Co Wyckoff sites: (simple dashed line) Co(0) in (2d); (Δ) Co(1) in (6h).

between β , φ and μ , λ can be understood because of the Mn-Mn distances with respect to the value of the Mn-Mn interaction (Fig. 7): In β , φ phases, medium-range environment of Va contains two Mn at distance 3.8 Å (Table II), whereas the smallest Mn(0)-Mn distance is 4.8 Å in μ , λ phases. According to the effective Mn-Mn interaction (Fig. 7), 3.8 Å corresponds to an unstable Mn-Mn distance, whereas 4.8 Å corresponds to a stable one.

The Al_5Co_2 phase is almost isomorphic to the β and φ phases, but there is a Co site [Co(0)] corresponding to the vacancy of β and φ (Table I). In this case $\Delta\mathcal{E}'_{\text{Co}(0)}$, calculated with the effective Co-Co interaction, is almost equal to $\Delta\mathcal{E}'_{\text{Co}(1)}$ (Fig. 10), thus Co(0) in (2d) is as stable as Co(1) in (6h). This shows why a vacancy does not exist in Al_5Co_2 . This analysis of the origin of the vacancy in terms of effective TM-TM interactions confirms the LMTO results presented in Sec. III D 2.

V. CONCLUSION

Both *ab initio* calculations of the density of states and a model to analyze the role of Mn atoms, have shown that a detailed analysis of the electronic structure explains the following features of $\beta\text{-Al}_9\text{Mn}_3\text{Si}$ and $\varphi\text{-Al}_{10}\text{Mn}_3$ atomic structures. Small amount of Si in $\beta\text{-Al}_9\text{Mn}_3\text{Si}$ stabilizes its structure thanks to a shift of the Fermi energy toward the

minimum of the pseudogap in the density of states (DOS). *Ab initio* DOS calculations shows that, at 0 K, Si atoms are on a specific Wyckoff site without mixed occupancy with some Al atoms.

$\beta\text{-Al}_9\text{Mn}_3\text{Si}$ and $\varphi\text{-Al}_{10}\text{Mn}_3$ are *spd*-Hume-Rothery phases. The transition metal (TM) elements have a crucial effect because *sp* electrons are strongly scattered by the Mn sublattice via the *sp-d* hybridization. As a result the electronic structure of Mn atoms and their stability depend strongly on the Mn positions. This effect is related to an effective Mn-Mn interaction which has a strong magnitude for Mn-Mn distances up to ~ 5 Å and more. This interaction is mediated by Al atoms and its medium-range character is due to a strong *sp*(Al)-*d*(Mn) hybridization. Thus, the pseudogap at Fermi energy comes from a combined effect of a Hume-Rothery mechanism and a strong *sp-d* hybridization. Recently, we have shown that the effective medium-range Mn-Mn interaction induces also pseudogap in Al_{12}Mn , $\alpha\text{-Al}_6\text{Mn}$, and $\alpha\text{-Al-Mn-Si}$.²⁵ Finally, both, density of states and effective TM-TM interactions lead to the understanding of the origin of a large vacancy existing in $\beta\text{-Al}_9\text{Mn}_3\text{Si}$ and $\varphi\text{-Al}_{10}\text{Mn}_3$, whereas similar sites are not vacant but occupied by Mn in $\mu\text{-Al}_{4,12}\text{Mn}$ and $\lambda\text{-Al}_4\text{Mn}$, and by Co in Al_5Co_2 .

To conclude, in $\beta\text{-Al}_9\text{Mn}_3\text{Si}$ phase and $\varphi\text{-Al}_{10}\text{Mn}_3$ phase, the Hume-Rothery minimization of band energy leads to a “frustration” mechanism which favors a complex atomic structure. A Mn sublattice appears to be the “skeleton” of the structure via the effective medium-range interactions between Mn atoms in the Al(Si) matrix. The β and φ structures are related to parts of the medium-range atomic order of quasicrystals and approximants. This suggests that a Hume-Rothery stabilization, expressed in terms of effective Mn-Mn interactions, might be intrinsically linked to the emergence of quasiperiodic structures in Al(Si)-Mn systems.

ACKNOWLEDGMENT

I am very grateful to D. Mayou with whom many ideas of this work have been developed. I also thank F. Hippert, M. Audier, D. Nguyen-Manh, R. Bellissent, V. Simonet, and J. J. Préjean for fruitful discussions. My thanks go to M. Audier and T.T. Truong for their careful reading of the manuscript.

*Electronic address: guy.trambly@ptm.u-cergy.fr

¹W. Hume-Rothery and G.V. Raynor, *The Structure of Metals and Alloys* (Institute of Metals, London, 1954).

²G.V. Raynor and M.B. Waldron, *Philos. Mag.* **40**, 198 (1949).

³A.M.B. Douglas, *Acta Crystallogr.* **3**, 19 (1950).

⁴A.D.I. Nicol, *Acta Crystallogr.* **6**, 285 (1953).

⁵G.V. Raynor, *Prog. Met. Phys.* **1**, 1 (1949).

⁶W. Hume-Rothery and B.R. Coles, *Adv. Phys.* **3**, 149 (1954).

⁷K. Robinson, *Acta Crystallogr.* **5**, 397 (1952).

⁸M.A. Taylor, *Acta Crystallogr.* **12**, 393 (1959).

⁹T.B. Massalski and U. Mizutani, *Prog. Mater. Sci.* **22**, 151 (1978).

¹⁰A.T. Paxton, M. Methfessel, and D.G. Pettifor, *Proc. R. Soc. London, Ser. A* **453**, 1493 (1997).

¹¹D.G. Pettifor, *The Science of Alloys for the 21st Century. A Hume-Rothery Symposium*, edited by P.E.A. Turchi, R.D. Shull, and A.

Gonis (Minerals, Metals, and Materials Society, Warrendale, 2000), pp. 121.

¹²J. Friedel, *Helv. Phys. Acta* **61**, 538 (1988).

¹³J. Friedel, *Philos. Mag. B* **65**, 1125 (1992).

¹⁴G. Trambly de Laissardière, D. Nguyen Manh, and D. Mayou, *Europhys. Lett.* **21**, 25 (1993).

¹⁵G. Trambly de Laissardière, D. Nguyen Manh, L. Magaud, J.P. Julien, F. Cyrot-Lackmann, and D. Mayou, *Phys. Rev. B* **52**, 7920 (1995).

¹⁶G. Trambly de Laissardière and D. Mayou, *Mater. Sci. Eng., A* **294-296**, 621 (2000).

¹⁷D. Nguyen Manh, G. Trambly de Laissardière, J.P. Julien, D. Mayou, and F. Cyrot-Lackmann, *Solid State Commun.* **82**, 329 (1992).

¹⁸M. Krajčič and J. Hafner, *J. Phys.: Condens. Matter* **14**, 5755

- (2002); **14**, 7201 (2002).
- ¹⁹A. Blandin, *Alloying Behaviour and Effects of Condensed Solid Solutions*, edited by T.B. Massalski (Gordon and Breach, New York, 1963); A. Blandin, *Phase Stability in Metals and Alloys*, edited by P.S. Rudman, J. Stringer, and R.I. Jaffee (McGraw-Hill, New York, 1967); A. Blandin, *Phys. Bull.* **31**, 93 (1980).
- ²⁰J. Hafner and L. von Heimendahl, *Phys. Rev. Lett.* **42**, 386 (1979).
- ²¹J. Hafner, *From Hamiltonians to Phase Diagrams* (Springer Verlag, Berlin, 1987).
- ²²D. Mayou, *Lecture on Quasicrystals* edited by F. Hippert and D. Gratias (Les Editions de Physique, Les Ulis, 1994), pp. 417-462.
- ²³J. Zou and A.E. Carlsson, *Phys. Rev. Lett.* **70**, 3748 (1993).
- ²⁴J. Zou and A.E. Carlsson, *Phys. Rev. B* **50**, 99 (1994).
- ²⁵G. Trambly de Laissardière, D. Nguyen-Manh, and D. Mayou, cond-mat/0209458 (unpublished).
- ²⁶G. Trambly de Laissardière and D. Mayou, *Phys. Rev. Lett.* **85**, 3273 (2000).
- ²⁷G. Trambly de Laissardière, D. Mayou, V. Simonet, F. Hippert, M. Audier, and R. Bellissent, *J. Magn. Magn. Mater.* **226-230**, 1029 (2001).
- ²⁸G. Trambly de Laissardière and D. Mayou, *Quasicrystals, an introduction to Structure, Physical Properties and Applications*, edited by J.B. Suck, M. Schreiber, and P. Häussler (Springer-Verlag, Berlin, 2002), pp. 487-504.
- ²⁹J.B. Newkirk, P.J. Black, and A. Damjanovic, *Acta Crystallogr.* **14**, 532 (1961).
- ³⁰S. Song and E.R. Ryba, *Philos. Mag. Lett.* **65**, 85 (1992).
- ³¹C.B. Shoemaker, D.A. Keszler, and D.P. Shoemaker, *Acta Crystallogr.* **45**, 13 (1989).
- ³²G. Kreinier and H.F. Franzen, *J. Alloys Compd.* **261**, 83 (1997).
- ³³G. Kreiner and H.F. Franzen, *J. Alloys Compd.* **221**, 15 (1995).
- ³⁴C. Berger, *Lecture on Quasicrystals*, edited by F. Hippert and D. Gratias (Les Editions de Physique, Les Ulis, 1994), pp. 463-504.
- ³⁵M. Hamerlin, S. Maamar, S. Fries, and H.L. Lukas, *Z. Metallkd.* **85**, 814 (1984).
- ³⁶V. Khare, R.S. Tiwari, and O.N. Srivastava, *Mater. Sci. Eng., A* **304-306**, 839 (2001).
- ³⁷A. Quivy, M. Quiquandon, Y. Calvayrac, F. Faudot, D. Gratias, C. Berger, R.A. Brand, V. Simonet, and F. Hippert, *J. Phys.: Condens. Matter* **8**, 4223 (1996).
- ³⁸T. Takeuchi, H. Yamada, M. Takata, T. Nakata, N. Tanaka, and U. Mizutani, *Mater. Sci. Eng., A* **294-296**, 340 (2000).
- ³⁹R. Tamura, T. Asao, and S. Takeuchi, *Phys. Rev. Lett.* **86**, 3104 (2001).
- ⁴⁰U. von Barth and L. Hedin, *J. Phys. C* **5**, 1629 (1972).
- ⁴¹O.K. Andersen, *Phys. Rev. B* **12**, 3060 (1975); O.K. Andersen, O. Jepsen, and D. Glötzel, *Highlights of Condensed Matter Theory*, edited by F. Bassani, F. Fumi, and M.P. Tosi (North-Holland, New York, 1985).
- ⁴²H.L. Skriver, *The LMTO Method* (Springer, New York, 1984).
- ⁴³O. Jepsen and O.K. Andersen, *Solid State Commun.* **9**, 1763 (1971).
- ⁴⁴In ASA, orbitals are introduced in vacancies so as to get a good expansion of the muffin tin orbitals out of atomic spheres (Refs. 41,42).
- ⁴⁵E. Belin-Ferrè, *J. Phys.: Condens. Matter* **14**, R789 (2002).
- ⁴⁶E. Belin-Ferrè, G. Trambly de Laissardière, P. Pêcheur, A. Sadoc, and J.M. Dubois, *J. Phys.: Condens. Matter* **9**, 9585 (1997).
- ⁴⁷M. Mori, S. Matsuo, T. Ishimasa, T. Matsuura, K. Kamiya, H. Inokuchi, and T. Matsukawa, *J. Phys.: Condens. Matter* **3**, 767 (1991).
- ⁴⁸E. Belin, J. Kojnok, A. Sadoc, A. Traverse, M. Harmelin, C. Berger, and J.M. Dubois, *J. Phys.: Condens. Matter* **4**, 1057 (1992).
- ⁴⁹Z. Dankhazi, G. Trambly de Laissardière, D. Nguyen-Manh, E. Belin, and D. Mayou, *J. Phys.: Condens. Matter* **9**, 3339 (1993).
- ⁵⁰T. Fujiwara, *Phys. Rev. B* **40**, 942 (1989); T. Fujiwara, S. Yamamoto, and G. Trambly de Laissardière, *Phys. Rev. Lett.* **71**, 4166 (1993).
- ⁵¹G. Trambly de Laissardière and T. Fujiwara, *Phys. Rev. B* **50**, 5999 (1994).
- ⁵²J. Hafner and M. Krajčič, *Phys. Rev. B* **57**, 2849 (1998).
- ⁵³M. Krajčič, M. Windisch, J. Hafner, G. Kresse, and M. Mihalkovic, *Phys. Rev. B* **51**, 17 355 (1995).
- ⁵⁴D. Mayou, *Phys. Rev. Lett.* **85**, 1290 (2000).
- ⁵⁵G. Trambly de Laissardière and D. Mayou, *Phys. Rev. B* **55**, 2890 (1997); G. Trambly de Laissardière, S. Roche, and D. Mayou, *Mater. Sci. Eng., A* **226-228**, 986 (1997).
- ⁵⁶D. Gratias, F. Puyraimond, M. Quiquandon, and A. Katz, *Phys. Rev. B* **63**, 024202 (2001).
- ⁵⁷J. Dolinšek, M. Klanjšek, T. Apih, A. Smontara, J.C. Lasjaunias, J.M. Dubois, and S.J. Poon, *Phys. Rev. B* **62**, 8862 (2000).
- ⁵⁸E.S. Zijlstra and T. Janssen, *Europhys. Lett.* **52**, 578 (2000).
- ⁵⁹Z.M. Stadnik, D. Purdie, M. Garnier, Y. Baer, A.P. Tsai, A. Inoue, K. Edagawa, S. Takeuchi, and K.H.J. Buschow, *Phys. Rev. B* **55**, 10 938 (1997).
- ⁶⁰Z.M. Stadnik, D. Purdie, Y. Baer, and T.A. Lograsso, *Phys. Rev. B* **64**, 214202 (2001).
- ⁶¹R. Phillips, J. Zou, A.E. Carlsson, and M. Widom, *Phys. Rev. B* **49**, 9322 (1994).
- ⁶²J.A. Moriarty and M. Widom, *Phys. Rev. B* **56**, 7905 (1997).
- ⁶³M. Mihalkovič, W.J. Zhu, C.L. Henley, and R. Phillips, *Phys. Rev. B* **53**, 9021 (1996).
- ⁶⁴M. Mihalkovič, H. Elhor, and J.B. Suck, *Phys. Rev. B* **63**, 214301 (2001).
- ⁶⁵E. Babić, R. Krsnik, B. Leontić, Z. Vučić, I. Zorić, and C. Rizuto, *Phys. Rev. Lett.* **27**, 805 (1971).
- ⁶⁶P.G. de Gennes, *J. Phys. Radium* **23**, 630 (1962).
- ⁶⁷P. Villars and L.D. Calvert, *Pearson's Handbook of Crystallographic Data for Intermetallic Phases* (American Society of Metals, Materials Park, OH, 1991), Vol. 1.
- ⁶⁸P. Guyot and M. Audier, *Philos. Mag.* **B 52**, L15 (1985).
- ⁶⁹V. Elser and C.L. Henley, *Phys. Rev. Lett.* **55**, 2883 (1985).